

## Transgenic Research

1  
2  
3 Metabolic engineering of astaxanthin biosynthesis in maize endosperm and characterization  
4 of a prototype high oil hybrid

5  
6 Gemma Farré<sup>1</sup>, Laura Perez-Fons<sup>2</sup>, Mathilde Decourcelle<sup>3</sup>, Jürgen Breitenbach<sup>4</sup>, Sonia Hem<sup>3</sup>,  
7 Changfu Zhu<sup>1</sup>, Teresa Capell<sup>1</sup>, Paul Christou<sup>1,5</sup>, Paul D. Fraser<sup>2</sup>, Gerhard Sandmann<sup>4\*</sup>

8  
9 <sup>1</sup>Department of Plant Production and Forestry Science, University of Lleida-Agrotecnio  
10 Center, Lleida, Spain

11 <sup>2</sup>School of Biological Sciences, Royal Holloway, University of London, Egham, Surrey, UK

12 <sup>3</sup>Unité de Biochimie et Physiologie Moléculaire des Plantes, INRA Montpellier, France

13 <sup>4</sup>Biosynthesis Group, Molecular Biosciences, Goethe University Frankfurt, Frankfurt,  
14 Germany

15 <sup>5</sup>Catalan Institute for Research and Advanced Studies (ICREA), Barcelona, Spain

16

17

18 \*Corresponding author at: Institute of Molecular Biosciences, Goethe University Frankfurt/M,  
19 Max von Laue Str. 9, D-60438 Frankfurt, Germany. Tel.: +49 69 798 29625; fax: +49 69 798  
20 29600.

21 E-mail address: sandmann@bio.uni-frankfurt.de

22

23

24

25 Key Words: astaxanthin; genetically engineered carotenoid biosynthesis; GM maize;  
26 metabolomics; transcriptomics

27

28

**Abstract**

29  
30 Maize was genetically engineered for the biosynthesis of the high value carotenoid  
31 astaxanthin in the kernel endosperm. Introduction of a  $\beta$ -carotene hydroxylase and a  $\beta$ -  
32 carotene ketolase into a white maize genetic background extended the carotenoid pathway to  
33 astaxanthin. Simultaneously, phytoene synthase, the controlling enzyme of carotenogenesis,  
34 was over-expressed for enhanced carotenoid production and lycopene  $\epsilon$ -cyclase was knocked-

1 down to direct more precursors into the  $\beta$ -branch of the extended ketocarotenoid pathway  
2 which ends with astaxanthin. This astaxanthin-accumulating transgenic line was crossed into  
3 a high oil- maize genotype in order to increase the storage capacity for lipophilic astaxanthin.  
4 The high oil astaxanthin hybrid was compared to its astaxanthin producing parent. We report  
5 an in depth metabolomic and proteomic analysis which revealed major up- or down-  
6 regulation of genes involved in primary metabolism. Specifically, amino acid biosynthesis  
7 and the citric acid cycle which compete with the synthesis or utilization of pyruvate and  
8 glyceraldehyde 3-phosphate, the precursors for carotenogenesis, were down-regulated.  
9 Nevertheless, principal component analysis demonstrated that this compositional change is  
10 within the range of the two wild type parents used to generate the high oil producing  
11 astaxanthin hybrid.

12

13

## 14 **Introduction**

15

16 Carotenoids are found in all groups of organisms with the exception of animals (Goodwin  
17 1980) which have to supply their carotenoid demand from their diet. Biosynthesis of  
18 carotenoids other than  $\beta$ -carotene can be specific for certain families or even species.

19 Carotenoids are present in all photosynthetic organisms. They protect against peroxidative  
20 processes (Krinsky 1989) and in animals they represent an essential source for vitamin A.  
21 Furthermore, color conferred by carotenoids is an aesthetic attractant (Vershinin 1999).

22 The animal feed and food coloring sectors dominate the global carotenoid market  
23 (Tyczkowski and Hamilton 1986). Although natural sources of carotenoids are available and  
24 are used especially in poultry feeding, the market is dominated by chemically synthesized  
25 carotenoids (Sandmann 2015; Berman et al. 2015). Attempts have been made to develop and  
26 establish biological systems for carotenoid production which can commercially compete with  
27 chemical synthesis. This is especially attractive for astaxanthin which is the highest-priced  
28 carotenoids on the market and is used as a feed additive in salmon farming (Tyczkowski and  
29 Hamilton 1986). The only known natural sources for astaxanthin are a few bacteria, some  
30 green algae, one fungal species and plants belonging to the genus *Adonis* (Goodwin 1980).  
31 Currently, the green alga *Haematococcus* and *Paracoccus carotinifaciens* are the only  
32 exploited natural astaxanthin sources (Ambati et al. 2014) but production costs are high and  
33 capacity low. Genetic engineering of an astaxanthin-producing organism for higher yields or  
34 the extension of carotenoid biosynthesis to astaxanthin are two promising strategies

1 (Sandmann 2001). The first approach has been followed recently with the fungus  
2 *Xanthophyllomyces dendrorhous* (Gassel et al. 2014). Starting from a chemically induced  
3 mutant with already increased astaxanthin synthesis, limiting genes for carotenogenic  
4 reactions were over-expressed stepwise to generate a highly astaxanthin producing strain.  
5 Genetic engineering of astaxanthin high-level accumulation in a crop plant was most  
6 successful with a  $\beta$ -carotene forming tomato variety by extension of the pathway mediated by  
7 hydroxylase and ketolase transgenes (Huang et al. 2013).

8 In this study, our engineering approach involved the establishment of high carotenoid  
9 biosynthesis in a pathway ending with astaxanthin in maize seed endosperm by multigene  
10 transformation. The maize seeds can be used directly as feed additives. Engineering of high  $\beta$ -  
11 carotene maize was already described (Zhu et al. 2008)). Feeding chickens on this maize as  
12 sole pigment source resulted in superior pigmentation due to accumulation of carotenoids in  
13 muscle and skin including a higher vitamin A content as well as much improved tolerance to a  
14 pathogen which constraints poultry production if not treated with antibiotics (Nogareta et al.  
15 2015). For better storage and extraction of astaxanthin, we chose a high-oil maize line to  
16 generate a prototype astaxanthin production line for further development. Here we report the  
17 generation and characterization of this line at the metabolome and proteome levels and  
18 conclude that even though perturbations in a number of primary metabolism pathways were  
19 identified, these were within the natural variation range in the parental lines.

20

21

## 22 **Materials and methods**

23

### 24 **Maize material**

25

26 Corn (*Zea mays*) variety M37W (white endosperm) was obtained from CSIR, Pretoria, South  
27 Africa. High-oil variety NSL 30876 referred to as NSL76 in this manuscript was kindly  
28 provided by USDA, ARS, NCRPIS, Iowa State University, Regional Plant Introduction  
29 Station, Ames, Iowa, USA. Both varieties, the selected transgenic line and the crosses were  
30 grown in the greenhouse at 28/20°C day/night temperature with a 10h photoperiod and 60-  
31 90% relative humidity during the first 50 days, followed by maintenance at 21/18°C day/night  
32 temperature with a 16h photoperiod thereafter. Transgenic line M37W-bkt with the modified  
33 carotenoid pathway to synthesize astaxanthin was out-crossed with NSL76 resulting in line  
34 NSL76-bkt. Homozygous T2 and T3 generations were derived by selfing. Endosperm samples

1 from immature seeds collected at 30 days after pollination (DAP) were frozen in liquid  
2 nitrogen and stored at  $-80^{\circ}\text{C}$  prior to use.

3

4 Vector construction and transformation

5

6 The phytoene synthase 1 cDNA (*PSY1*) was cloned from inbred maize line B73 by RT-PCR  
7 with forward primer 5'-AGGATCCATGGCCATCATACTCGTACGAG-3' with *Bam*HI site  
8 (underlined) and reverse primer 5'-AGAATTCTAGGTCTGGCCATTTCTCAATG-3' with  
9 *Eco*RI site (underlined). Plasmid p326-ZmPSY1 (Zhu et al. 2008) is under the control of the  
10 LMW glutenin promoter (Colot et al. 1987). A maize lycopene  $\epsilon$ -cyclase (*LYCE*) cDNA  
11 fragment was amplified by RT-PCR with ZmLYCE cDNA as template using forward (5'-  
12 GGAATTCTCTAGACGATCTCGGCGCCGCTCGGCTGCT-3') with *Eco*RI and *Xba*I sites  
13 (underlined) and reverse primers (5'-gactagtggatcccaatgagacctacagtgagacct-3') with *Spe*I and  
14 *Bam*HI sites based on sequence information in GenBank (accession numbers EF622043). This  
15 sense DNA was cloned into the pHorP vector (Sørensen et al. 1996) containing the barley D-  
16 hordein promoter with a 300 bp *gusA* gene fragment and the ADP-glucose pyrophosphorylase  
17 terminator via restriction with *Xba*I and *Bam*HI and the antisense *LYCE* fragment into the  
18 *Spe*I and *Eco*RI sites. The chemically synthesized truncated *Chlamydomonas reinhardtii*  $\beta$ -  
19 carotene ketolase gene (*sCrBKT*) (Zhong et al. 2011) fused to the pea small subunit of  
20 Rubisco (*SSU*) (Schreier et al. 1985) and 5'-untranslated region (5'UTR) of the rice alcohol  
21 dehydrogenase gene (Sugio et al. 2008) was inserted into pGZ63 vector (Zhu et al. 2008)  
22 between the maize  $\gamma$ -zein promoter and nos terminator using the *Bam*HI and *Sac*I restriction  
23 sites. The *CrBKT* and *SSU* codon usage was modified to a monocotyledonous plant  
24 preference. The *CRTZ* gene encoding beta-carotene hydroxylase from *Brevundimonas* sp.  
25 Strain SD212 (MBIC 03018) (Nishida et al. 2005) was chemically synthesized according to  
26 the codon usage of *Brassica napus* (accession number AB377272) and kindly provided by Dr.  
27 Norihiko Misawa, Ishikawa Prefectural University, Japan. The *sBrCRTZ* gene fused with the  
28 pea small subunit of Rubisco (*SSU*) and 5'-untranslated region (5'UTR) of the rice alcohol  
29 dehydrogenase gene was digested with *Bam*HI and *Sac*I. The digested fragments were cloned  
30 into the *Bam*HI and *Sac*I site of pGZ63 with the maize  $\gamma$ -zein gene promoter to generate  
31 pGZ63-sBrCRTZ. The *bar* gene encoding phosphinothricin N-acetyltransferase (Thompson et  
32 al. 1987) was used as a selectable marker. Details of the final plasmids can be found in Fig.  
33 1A. The procedure used for transformation of M37W maize was described in Zhu et al.  
34 (2008). The highest-accumulating astaxanthin M37W-bkt lines were crossed with a high oil

1 line (NSL76) to generate NSL76-bkt, which is the subject of the in depth metabolomic and  
2 proteomic analysis reported in this manuscript.

3

4 Transcript analysis

5

6 Total RNA (30 µg) was fractionated on a denaturing 1.2% (w/v) agarose gel containing  
7 formaldehyde prior to blotting. The membrane was probed with digoxigenin-labeled partial  
8 cDNAs prepared as above using the PCR-DIG Probe Synthesis Kit (Roche, Mannheim,  
9 Germany), with hybridization carried out at 50°C overnight using DIG Easy Hyb. The  
10 membrane was washed twice for 5 min in 2x SSC, 0.1% SDS at room temperature, twice for  
11 20 min in 0.2x SSC, 0.1% SDS at 68°C, and then twice for 10 min in 0.1x SSC, 0.1% SDS at  
12 68°C. After immunological detection with anti-DIG-AP (Fab-Fragments Diagnostics GmbH,  
13 Germany) chemo luminescence generated by disodium 3-(4-methoxyspiro {1,2-dioxetane-  
14 3,2'-(5'-chloro)tricyclo[3.3.1.1<sup>3,7</sup>] decan}-4-yl) phenyl phosphate (CSPD) (Roche, Mannheim,  
15 Germany) was detected on Kodak BioMax light film (Sigma-Aldrich, USA) according to the  
16 manufacturer's instructions.

17 Primers for the probes were Zmpsy1-forward 5'-GTGTAGGAGGACAGATGAGCTTGT-3',  
18 Zmpsy1-reverse 5'-CATCTGCTAGCCTGTGAGAGCTCA-3', CrBKT-forward 5'-  
19 GGATCCTCAGCCAGGAGCCAGTGCAGCGCCTCT-3', CrBKT-reverse 5'-  
20 GAATTCATGGGGCCAGGCATTCAGCCCACTTCCG-3', sBrCRTZ-forward 5'-  
21 ACGAATTCGATGGCCTGGCTGACGT -3', sBrCRTZ-reverse 5'-  
22 TAGAGGATCCTCAGGCGCCGCTGCTGG-3', GUS-forward 5-  
23 GGTCTAGAGGATCCGCACCTCTGGCAACCGGGTGAAGGT-3', GUS-reverse 5-  
24 GTGAATTCAGTAGTCGAGCATCTCTTCAGCGTAAGGGTAA-3'.

25

26 Quantitative real time PCR

27

28 Real-time PCR was performed on a BIO-RAD CFX96<sup>TM</sup> system using 25µl mixture  
29 containing 10 ng of synthesized cDNA, 1X iQ SYBR green supermix (BIO-RAD) and 0.2  
30 mM forward and reverse primer concentrations. Primers for maize endogenous lycopene ε-  
31 cyclase gene are 5'- AGTCCATCAATGCTTGCATGG -3' (forward primer) and 5'-  
32 CATCTCGGCACCCTGAAAAAG -3' (reverse primer). Primers for the internal control actin gene  
33 are 5'- CGATTGAGCATGGCATTGTCA -3' (forward primer) and 5'- CCCACTAGCGTACAACGAA  
34 -3' (reverse primer). To enable calculation of relative expression levels, serial dilutions (125

1 ng to 0.2 ng) were used for the generation of standard curves for each gene separately. PCR  
2 reactions were performed in triplicate using 96-well optical reaction plates. Cycling  
3 conditions consisted of a single incubation step at 95°C for 5 min, followed by 40 cycles of  
4 95°C for 0:15 min, 58°C for 1 min, 72°C for 0:20 min. Specificity of amplification was  
5 confirmed by melt curve analysis of final PCR products with a temperature range of 50°C to  
6 90 °C with fluorescence acquired after every 0.5°C increase. The fluorescence threshold value  
7 and gene expression data were calculated using the CFX96™ system software. Values  
8 represent the mean of three RT-PCR replicates  $\pm$  SD.

### 9 10 11 Carotenoid analysis

12  
13 The powdered seeds and endosperm samples were extracted with tetrahydrofurane/methanol  
14 (50:50, v/v) by heating for 20 min. at 60°C and then partitioned into 30% ether in petrol. The  
15 collected upper phase was evaporated and re-dissolved in acetone for high-performance liquid  
16 chromatography (HPLC) analysis on a 15 cm Nucleosil C18, 3µm column with a mobile  
17 phase of acetonitrile/2-propanol/methanol/ (85:5:10, v/v/v). The flow was 1 ml/min, at 20°C  
18 column temperature. Spectra were recorded online with a photodiode array detector 440  
19 (Kontron, Straubenhard, Germany). Identification and quantification was performed by co-  
20 chromatography and comparison of spectral properties with authentic standards and reference  
21 spectra (Britton et al. 2004).

### 22 23 Metabolome analysis

24  
25 General metabolite profiling of polar and non-polar metabolites from freeze-dried maize  
26 endosperm powder was performed as described recently (Decourcelle et al. 2015). After  
27 methanol extraction and addition of the internal standard ribitol, samples were derivatized  
28 with methoxyamine-HCl (Sigma-Aldrich) and N-methyltrimethylsilyltrifluoroacetamide  
29 (Macherey Nagel). Gas chromatography–mass spectrometry analysis was performed on an  
30 Agilent 7890A gas chromatograph with a 5975 MSD. For components identification, an in-  
31 house mass spectral library constructed from standards as well as the NIST 98MS library  
32 (Perez-Fons et al. 2014) were used. Quantification and identification were achieved using  
33 AMDIS (v 2.71) software facilitating integrated peak areas for specific compound targets  
34 (qualifier ions) relative to the ribitol internal standard peak. Data matrices were transformed

1 using the pareto-scaled method (van den Berg et al., 2006) and multivariate analysis  
2 performed using SIMCA-P+ 12.0 (Umetrics AB, Sweden). Pathway diagrams were created  
3 using the in-house developed software BioSynlab<sup>®</sup> (Royal Holloway, University of London)  
4 or Powerpoint. Means, standard deviation, p-values and q-values were calculated in Excel.

5

## 6 Proteome analysis

7

8 Proteome analysis included protein fractionation, tryptic digestion, peptide separation, and  
9 analysis by tandem mass spectrometry. Proteins of ground maize endosperms were extracted  
10 and proteins separated as recently described (Decourcelle et al. 2015). Mass spectrometric  
11 analysis was carried out with a Q-TOF mass spectrometer (Maxis Impact, Bruker Daltonics)  
12 with a Captive Spray ion source interfaced with a nano-LC Ultimate 3000 (Thermo Scientific)  
13 at a flow rate of 20  $\mu$ L/min using 0.1% formic acid and separated with a reversed-phase  
14 capillary column (C18 PepMan10, 75  $\mu$ m x 250 mm, 3  $\mu$ m, 100A, Thermo Scientific) at a  
15 flow rate of 0.3  $\mu$ L/min using a two steps gradient (8% to 28% ACN with 0.1% formic acid in  
16 40 min then 28% to 42% in 10 min), and eluted directly into the mass spectrometer.

17 Proteins were identified by MS/MS by data-dependent acquisition of fragmentation  
18 spectra of multiple charged peptides using Data Analysis software (Bruker Daltonics GmbH,  
19 Bremen, Germany) to generate peak lists. Protein identification was obtained by searching  
20 with X!Tandem (version 2013.09.01; <http://www.thegpm.org/tandem/>) against the  
21 Maizesequence.org (release AGPv3.21) and UniProtKB (maize taxonomy) (release 2014\_03)  
22 combined database, using carbamidomethylation of cysteine as fixed modification, and N-  
23 terminus acetylation, deamidation of asparagine and glutamine, oxidation of methionine, and  
24 phosphorylation of serine, threonine and tyrosine as variable modifications. The functional  
25 annotations of proteins (GO) were established with MSDA (Mass Spectrometry Data Analysis,  
26 <https://msda.unistra.fr/>, Carapito et al. 2014).

27 Label-free quantification was carried out with the MassChroQ software (version 2.1)  
28 (Valot et al. 2011) based on extracted ion chromatograms. The detection threshold on min and  
29 max were set at 3000 and 5000, respectively. Data were filtered to remove (i) unreliable  
30 peptides for which standard deviation of retention time was superior to 60 seconds, (ii)  
31 peptides shared by several proteins and (iii) quantified peptides in less than 3 biological  
32 replicates. Normalization was performed to take into account possible global quantitative  
33 variations between LC-MS runs. Normalized peptide areas were calculated by dividing the  
34 area value of each peptide by the sum of all peptide area values for each LC-MS. Since a

1 peptide can be detected in several SDS-PAGE bands, peptide abundance in one sample is  
2 calculated by summing the normalized areas of this peptide in each of these bands. And  
3 protein abundance was calculated by summing the normalized peptide area. Univariate  
4 differential analysis was performed with the more appropriate statistical test, Wilcoxon test  
5 (control of the normality and homoscedasticity hypotheses) with the "multi-test" package  
6 ('R/Bioconductor' statistical open source software. Multiple testing corrections enabled to  
7 adjust the p-value of each marker to control the false discovery rate with the "multi-test"  
8 package ('R/Bioconductor' statistical open source software). Protein fold change was  
9 calculated after averaging protein areas between the biological replicates.

## 12 **Results**

### 14 Generation of astaxanthin maize lines

16 Our strategy for engineering a high-oil astaxanthin producing maize transformant is outlined  
17 in Fig. 1. It started with M37W as a suitable and efficient transformation host and the  
18 breeding of the engineered astaxanthin pathway into the high-oil NSL76 line. Starting with  
19 the wild type white endosperm M37W, genetic transformation was carried out with additional  
20 copies of the endogenous phytoene synthase 1, together with the bacterial  $\beta$ -carotene  
21 hydroxylase (*crtZ*) and algal  $\beta$ -carotene ketolase genes codon optimized for maize. Since  
22 astaxanthin is directly derived from zeaxanthin via  $\beta$ -carotene, and NSL76 possess an active  
23 alternative route to lutein, an antisense construct of lycopene  $\epsilon$ -cyclase was additionally  
24 included in the transformation (Fig. 1A) in order to divert lycopene preferentially into the  $\beta$ -  
25 branch of the carotenoid pathway. M37-bkt was selfed to generate lines which were used to  
26 breed with the high oil NSL76 line. The experimental strategy for the introgression of the  
27 modified carotenoid pathway into NSL76 yielding NSL76-bkt is shown in Fig. 1B.

### 29 Expression of carotenogenic genes

31 Transcript analysis for the expressed carotenogenic genes was carried out by mRNA blot  
32 analysis of the transgenes (Fig. 2). The *ZmPSY1* transcript was not detectable in wild-type  
33 M37W endosperm, in agreement with previous investigations (Zhu et al. 2008), but it was  
34 expressed in the rest of the lines. The highest *ZmPSY1* expression levels were observed in



1 NSL76-bkt. *sBrCRTZ*, and *CrBKT* were expressed in the transgenic line and the crosses,  
2 although at different levels. Each transgene was expressed at similar levels in the transgenic  
3 line and the crosses and no expression was detected in the two wild-types M37W and NSL76.  
4 Amounts of the endogenous *Zmlyce* gene which was down-regulated by transformation with  
5 RNAi-LYCE were determined by quantitative real-time PCR in all four maize lines (Fig. 3).  
6 In both transformants M37-bkt and NSL76-bkt, the levels were only about one sixth  
7 compared to the corresponding non-transformed lines, M37 and NSL76.

8

### 9 Carotenoid content and metabolite profiling

10

11 Due to the use of endosperm specific promoters, carotenoids were analysed from endosperm  
12 and whole seeds of the initial line M37W, the M37-bkt transformant, the high oil line NSL76  
13 and the NSL76-bkt hybrid (Table 1). The results demonstrate that M37W is low in  
14 carotenoids and only violaxanthin, lutein and zeaxanthin were detectable. The same  
15 carotenoids were found in the seeds of the other wild type NSL76 but with much higher  
16 concentrations of lutein. In NSL76 trace amounts of the lutein and zeaxanthin precursors  $\alpha$ -  
17 cryptoxanthin and  $\beta$ -cryptoxanthin were detectable. In the transformant M37-bkt and the  
18 cross NSL76-bkt the two ketocarotenoids astaxanthin and 4-ketozeaxanthin were present in  
19 addition to  $\beta$ -carotene. Astaxanthin was the predominant carotenoid in M37-bkt as well as in  
20 NSL76-bkt. Astaxanthin concentrations in endosperm and whole seeds were in the same  
21 range in the two lines.

22 For the analysis of global metabolite changes of the final line NSL76-bkt versus its  
23 parent line NSL76, metabolite profiling of the intermediary metabolism was carried out with a  
24 GCMS platform (Enfissi et al. 2010; Perez-Fons et al. 2014) which enables detection of most  
25 of the compound of maize intermediary metabolism (Decourcelle et al. 2015). Only the  
26 concentrations of sucrose and lactic acid were significantly increased (by more than 10-fold)  
27 (Table 2) whilst other metabolite pools were significantly decreased. These included mainly  
28 amino acids of the pyruvate family that is leucine, alanine and valine as well as serine and  
29 glycine and metabolically related glyceric acid. Furthermore, metabolites connected to the  
30 citric acid cycle were lower in NSL76-bkt. These comprise fumaric, malic and succinic acid  
31 together with amino acids of the aspartate (aspartic acid and threonine) and of the glutamate  
32 families (glutamic acid and proline).

33 Principal component analysis (PCA) of intermediary metabolism of the four lines  
34 described in this study was carried out in order to assess the effect of keto carotenoid

1 accumulation on intermediary metabolism. PCA components 1 and 2 explain 61.8 and 17.7%  
2 of the variability, respectively, and their corresponding score and loadings plots are shown in  
3 Fig. 4. The four lines separate out in the PCA score plot (Fig. 4A) indicating differences in the  
4 intermediary metabolism between groups of samples. The homozygous red endosperm line  
5 NSL76-bkt clusters closer to the M37W group (wild type) and away from its parental lines  
6 NSL76 and M37-bkt. The results in the loadings plot (Fig. 4B) indicate that sucrose, glucose  
7 and methyl galactose are responsible for the clustering of NSL76-bkt and M37W in the PCA  
8 score plot.

### 9 10 Proteomic profiling

11  
12 Proteomic profiling was carried out with endosperm from seeds harvested 30 DAP and of MS  
13 from NSL76 and NSL76-bkt lines. Using the decoy database and the tolerated presence of at  
14 least 2 peptides with an e-value smaller than 0.05 and a protein e-value smaller than 0.0001,  
15 the false discovery rate was 0.13% and 0.23%, respectively, for peptide and protein  
16 identification for 30 DAP samples, and 0.12% and 0.17%, respectively, for the MS samples.  
17 Our approach allowed the identification of 1,688 non-redundant and grouped proteins at 30  
18 DAP and 1,220 at the MS stage. For data quantification, MassChroQ software was used and  
19 proteins with significant quantitative change, NSL76-bkt versus NSL-76, (Wilcoxon p-value  
20  $<0.05$  AUC (area under curve)  $>0.9$ ) and with fold-change  $>1.5$ ) were considered. In MS, 14  
21 proteins varied in their abundance of which 3 were significantly increased and the others  
22 decreased. In endosperm of 30 DAP seeds, there were 17 variant proteins of which 4 were  
23 increased (Table 3).

24 In MS, an uncharacterized protein, stress-related peroxidase and acid phosphatase  
25 were found higher in NSL76-bkt maize compared to its parent line (Table 3A). Of the  
26 characterized proteins related to glycolysis, the amounts of sugars and amino acid metabolism,  
27 malate dehydrogenase, endochitinase and glutamine synthase were decreased. At 30 DAP, no  
28 metabolic pathway-related protein with higher concentrations in the astaxanthin accumulating  
29 transformant was detectable (Table 3B). Metabolic enzymes with lower abundance were 1,3-  
30 diphosphoglycerate phosphatase, trehalose-6-phosphate synthase and sucrose synthase. In  
31 addition, changes in storage proteins were observed with increased concentrations of a  
32 leguminin-like protein and a decrease of prolamin (Table 3B).

33

34

## 1 Discussion

2

3 Carotenoid synthesis in seeds of engineered and high oil hybrid maize lines

4

5 We had reported earlier a library of maize transformants constructed by transfer of  
6 carotenogenic genes under endosperm-specific promoters for increased carotenoid production  
7 in seed endosperm (Zhu et al. 2008). Among these a particular line with low astaxanthin  
8 content (about 3% of total carotenoids) was recovered. This proof of concept experiment  
9 encouraged us to select more suitable genes for a more efficient astaxanthin synthesis in  
10 maize. To overcome the problem of ketolase and hydroxylase competition during astaxanthin  
11 biosynthesis from  $\beta$ -carotene (Zhong et al. 2011), we transformed maize line M37W with  $\beta$ -  
12 carotene hydroxylase (*crtZ*) from *Brevundimonas* and  $\beta$ -carotene ketolase from  
13 *Chlamydomonas reinhardtii* which were shown to be highly efficient in tobacco (Hasunuma  
14 et al. 2008) and tomato (Huang et al. 2013). In order to enhance the pool of  $\beta$ -carotene as  
15 precursor of astaxanthin, we over-expressed phytoene synthase 1 (resulting in a 7 to 8-fold  
16 increase of total seed carotenoids) and knocked-down lycopene  $\epsilon$ -cyclase. The latter  
17 modification decreased the transcript levels (Fig. 3) which in turn shifted metabolite  
18 distribution into the  $\beta$  branch of the carotenoid pathway from which astaxanthin originates.  
19 This is indicated by the changing ratios of  $\beta$ -branch carotenoids (all except lutein and  $\alpha$ -  
20 carotene) versus the  $\epsilon$ -branch carotenoids (lutein plus  $\alpha$ -carotene) from 0.3 in M37W to 25 in  
21 the final NSL76-bkt line (Table 1). All modifications were monitored by mRNA blot analysis  
22 in M37-bkt and in NSL76-bkt (Fig. 2). After crossing of the astaxanthin pathway into the  
23 high-oil NSL76 line, astaxanthin accumulation in the seeds increased by ca. 50% (Table 1).  
24 This may be due to higher storage capacity for lipophilic compound in an oil environment,  
25 although only about 15% of the oil is stored in the endosperm (Hartings et al. 2012). NSL76-  
26 bkt accumulated 60% of whole seed carotenoids as astaxanthin and 45% of the endosperm  
27 carotenoids. This resembles a highly efficient astaxanthin biosynthesis pathway near the  
28 biosynthesis efficiency in transgenic tobacco (Hasunuma et al. 2008) and tomato (Huang et al.  
29 2013). Due to the high starch content of the seeds and the endosperm, the astaxanthin content  
30 in maize was lower compared to tomato. However, the combination of astaxanthin and starch  
31 content makes NSL76-bkt a useful feed component, e.g. for fish farming and for raising  
32 poultry.

33

34 Metabolism in seeds of NSL76-bkt

1  
2 The increase of total carotenoid content in M37W-bkt and NSL76-bkt (Table 1) is due to the  
3 over-expression of the phytoene synthase 1 gene which has been shown in different plant  
4 species to limit carotenoid synthesis (Sandman et al. 2006). The enhanced metabolite flow  
5 into the carotenoid pathway affects primary metabolism as a source for terpenoid pathway  
6 precursors in the transformants as already demonstrated for maize high in zeaxanthin and  
7 other carotenoids (Decourcelle et al. 2015). For NSL76 and NSL76-bkt, metabolic changes  
8 were analysed by comparing pool sizes of compounds and amounts of enzymes. Most evident  
9 was the increase of sucrose and lactate pools in the endosperm (Table 2). Maize kernels are  
10 supplied from the green parts of the plant with different sugars including sucrose (Alfonso et  
11 al. 2011). Sucrose can be further metabolized to glucose and fructose by invertase or to  
12 fructose and UDP-glucose by sucrose synthase as the initial reaction for starch synthesis  
13 (Spielbauer et al. 2006). The concentration of the latter enzyme was decreased providing less  
14 UDP-glucose for the synthesis of other sugars, including trehalose which is additionally  
15 supported by lower trehalose synthase concentrations in NSL76-bkt (Table 3B). These  
16 changes in enzyme amounts preferentially support glycolytic metabolism to the precursors for  
17 carotenoid biosynthesis. Lactate can be considered as a key compound for the provision of  
18 pyruvate together with glyceraldehyde 3-phosphate, the major substrates for the  
19 deoxyxylulose 5-phosphate pathway leading to terpenoids (Eisenreich et al. 2001). Lactate  
20 accumulation (Table 2) coincides with lower activities of pools of the citric acid cycle  
21 components and lower concentrations of malate dehydrogenase. This indicates a reduced flow  
22 of pyruvate into the citric acid cycle (Table 3A). It appears that pathways competing with  
23 glycolytic pyruvate formation or competing with the deoxyxylulose 5-phosphate pathway for  
24 pyruvate are down-regulated. This is also the case for decreased formation of glycerate out of  
25 the glycolytic pathway (Table 2). A similar down-regulation of starch biosynthesis, with a  
26 concurrent increase of the sucrose pool, also competing with glycolysis was found in an  
27 engineered high-carotenoid maize line (Decourcelle et al. 2015).

28 A very strong decrease of amino acid pools from most amino acid families was  
29 measured in NSL76-bkt (Table 2). This includes all amino acids derived from pyruvate which  
30 is needed for higher carotenoid synthesis. The concentration of a legumin-like protein was  
31 increased in the endosperm at 30 DAP (Table 3B). In this maize storage protein, the  
32 predominant amino acids are histidine and glutamine (Yamagata et al. 2003) which in contrast  
33 to several other amino acids remained unchanged in NSL76-bkt compared to NSL76. Unlike  
34 legumin, concentrations of prolamin, another storage protein were decreased in NSL76-bkt.

1 This may be due to lack of leucine, alanine and proline in NSL76-bkt (Table 2) which are the  
2 major amino acids in maize prolamins (Kim et al. 1988).

3 No characterized enzyme related to primary metabolism in endosperm either at 30  
4 DAP or in mature seeds was up-regulated in NSL76-bkt. The only enzyme present in higher  
5 concentration in NSL76-bkt was a peroxidase (Table 3A). In maize kernels, this enzyme is  
6 part of an antioxidative system to cope with oxidative stress (Corona-Carrillo et al. 2014)  
7 which seems to be enhanced in NSL76-bkt. Despite the variability in the metabolic profile of  
8 NSL76-bkt compared to NSL76, the principal component analysis (Fig. 4) indicated that the  
9 changes are within the natural variation of the two wild type varieties M37W and NSL76.

10

11

## 12 **Conclusion**

13

14 High astaxanthin accumulation in maize endosperm can be achieved by over-expression of  
15 the gene encoding phytoene synthase 1, the limiting enzyme of the pathway, knock-down of  
16 the competing  $\epsilon$ -branch and selection of interactive hydroxylase and ketolase genes.  
17 Metabolome and proteome analysis provided basic insights into how maize primary  
18 metabolism supports the synthesis of high levels of astaxanthin from pyruvate and  
19 glyceraldehyde 3-phosphate in the NSL76-bkt line by favouring the flow of these precursors  
20 into the glycolytic pathway. With this genetic engineering approach, we were successful in  
21 generating a staple crop as a source of corn oil containing the highly antioxidative carotenoid  
22 astaxanthin. This corn line can also be used directly as a feed to supply astaxanthin together  
23 with oil and carbohydrate e.g. in fish farming. Alternatively, NSL76-bkt can be used as a raw  
24 material for the extraction of an oily astaxanthin preparation which will form the basis for  
25 other industrial processes.

26

27

## 28 **Acknowledgements**

29

30 Funding through the Plant KBBE project CaroMaize is gratefully acknowledged. Further  
31 support to PC was by the Ministerio de Economía y Competitividad, Spain (BIO2014-54441-  
32 P, BIO2011-22525) and a European Research Council Advanced Grant (BIOFORCE);  
33 PROGRAMA ESTATAL DE INVESTIGACIÓN CIENTÍFICA Y TÉCNICA DE  
34 EXCELENCIA, Spain (BIO2015-71703-REDT). PDF and LP are grateful for funding from

1 the EU FP7 project DISCO grant number 613513. We thank Sys2Diag team (CNRS, France)  
2 for statistical analyses of proteomic data and particularly Nicolas Salvetat and Franck Molina  
3

## 1 **References**

2  
3  
4  
5  
6  
7  
8  
9  
10  
11  
12  
13  
14  
15  
16  
17  
18  
19  
20  
21  
22  
23  
24  
25  
26  
27  
28  
29  
30  
31  
32  
33  
34

- Ambati RR, Moi PS, Ravi S, Aswathanarayana RG (2014) Astaxanthin: Sources, extraction, stability, biological activities and its commercial applications - A review. *Mar Drugs* 12:128–152
- Alfonso AP, Val DL, Shachar-Hill T (2011) Central metabolic fluxes in the endosperm of developing maize seeds and their implications for metabolic engineering. *Metabolic Engin* 13:96–107
- Berman J, Zorrilla-López U, Farré G, Zhu C, Sandmann G, Twyman RM, Capell T, Christou C (2015) Nutritionally important carotenoids as consumer products. *Phytochem Rev* 14:727-743
- Britton G, Liaaen-Jensen S, Pfander H (2004) *Carotenoids Handbook*. Birkhäuser Verlag, Basel
- Carapito C, Burel A, Guterl P, Walter A, Varrier F, Bertile F, Van Dorsselaer A (2014). MSDA, a proteomics software suite for in-depth Mass Spectrometry Data Analysis using grid computing. *Proteomics* 14:1014-1019
- Colot V, Roberts LS, Kavanagh TA, Bevan MW, Thomson RD (1987) Localization of sequences in wheat endosperm protein genes which confer tissue-specific expression in tobacco. *EMBO J* 6:3559-3564
- Corona-Carrillo JI, Flores-Ponce M, Chávez-Nájera G, Díaz-Pontones DM (2014) Peroxidase activity in scutella of maize in association with anatomical changes during germination and grain storage. *SpringerPlus* 3:399
- Decourcelle M, Perez-Fons L, Baulande S, Steiger S, Couvelard L, Hem S, Zhu C, Capell T, Christou P, Fraser P, Sandmann G (2015) Combined transcript, proteome, and metabolite analysis of transgenic maize seeds engineered for enhanced carotenoid synthesis reveals pleiotropic effects in core metabolism. *J Exp Bot* 66:3141-3150
- Eisenreich W, Roj dich F, Bacher A (2001) Deoxyxylulose phosphate pathway to terpenoids. *Trends Plant Sc* 6:78-84
- Enfissi EM, Barneche F, Ahmed I, Lichtlé C, Gerrish C, McQuinn RP, Giovannoni JJ, Lopez-Juez E, Bowler C, Bramley PM, Fraser PD (2010) Integrative transcript and metabolite analysis of nutritionally enhanced DE-ETIOLATED1 downregulated tomato fruit. *Plant Cell* 22:1190-1215
- Gassel S, Breitenbach J, Sandmann G (2014) Genetic engineering of the complete carotenoid pathway towards enhanced astaxanthin formation in *Xanthophyllomyces*

- 1 *dendrorhous* starting from a high-yield mutant. Appl Microbiol Biotechnol 98:345-  
2 350
- 3 Goodwin TW (1980) The Biochemistry of the Carotenoids: Volume I Plants. Chapman and  
4 Hall, London
- 5 Hartings H, Fracassetti M, Motto M (2012) Access genetic enhancement of grain quality-  
6 related traits in maize. In: Transgenic Plants - Advances and Limitations, Çiftçi YÖ  
7 (Edit) InTech Publisher, pp. 191-218
- 8 Hasunuma T, Miyazawa SI, Yoshimura S, Shinzaki Y, Tomizawa KI, Shindo K, Choi SK,  
9 Misawa N, Miyake C (2008) Biosynthesis of astaxanthin in tobacco leaves by  
10 transplastomic engineering. Plant J 55:857-868
- 11 Huang JC, Zhong YJ, Liu J, Sandmann G, Chen F. (2013) Metabolic engineering of  
12 tomato for high-yield production of astaxanthin. Metab Eng 17:59-67
- 13 Nishida Y, Adachi K, Kasai H, Shizuri Y, Shindo K, Sawabe A, Komemushi S, Miki W,  
14 Misawa N (2005) Elucidation of a carotenoid biosynthesis gene cluster encoding a  
15 novel enzyme, 2,2'-beta-hydroxylase, from *Brevundimonas* sp. strain SD212 and  
16 combinatorial biosynthesis of new or rare xanthophylls. Appl Environ Microbiol  
17 71:4286-4296
- 18 Kim WT, Okita TW (1988) Structure, expression, and heterogeneity of the rice seed  
19 prolamines. Plant Physiol 88:649-655
- 20 Krinsky NI (1989) Antioxidant functions of carotenoids. Free Radic Biol Med 7: 617-635
- 21 Nogareda C, Moreno JA, Angulo E, Sandmann G, Portero M, Capell T, Zhu C, Christou P  
22 (2015) Carotenoid-enriched transgenic corn delivers bioavailable carotenoids to  
23 poultry and protects them against coccidiosis. Plant Biotechnol J [Epub ahead of  
24 print] PubMed
- 25 Perez-Fons L, Bramley PM, Fraser PD (2014) The optimisation and application of a  
26 metabolite profiling procedure for the metabolic phenotyping of *Bacillus* species.  
27 Metabolomics 10:77-90
- 28 Sandmann G (2001) Genetic manipulation of carotenoid biosynthesis: strategies, problems  
29 and achievements. Trends Plant Sci 6:14-17
- 30 Sandmann, G (2015) Carotenoids of biotechnological importance. In: Biotechnology of  
31 Isoprenoids, Schrader J, Bohlmann J (Edits) Springer-Verlag Berlin Heidelberg, pp  
32 449-467
- 33 Sandmann G, Römer S, Fraser PD (2006) Understanding carotenoid metabolism as a  
34 necessity for genetic engineering of crop plants. Metabolic Engin 8:291-302



- 1 Schreier PH, Seftor EA, Schell J, Bohnert HJ (1985) The use of nuclear-encoded  
2 sequences to direct the light-regulated synthesis and transport of a foreign protein  
3 into plant chloroplasts. *EMBO J* 4:25-32
- 4 Sørensen MB, Müller M, Skerritt J, Simpson D (1996) Hordein promoter methylation and  
5 transcriptional activity in wild-type and mutant barley endosperm. *Molec Gen  
6 Genetics* 250:750–760
- 7 Spielbauer G, Margl L, Hannah LC, Römisch W, Ettenhuber C, Bacher A, Gierl A,  
8 Eisenreich W, Genschel U (2006) Robustness of central carbohydrate metabolism  
9 in developing maize kernels. *Phytochem* 67:1460-1475
- 10 Sugio T, Satoh J, Matsuura H, Shinmyo A, Kato K (2008) The 5'-untranslated region of the  
11 *Oryza sativa* alcohol dehydrogenase gene functions as a translational enhancer in  
12 monocotyledonous plant cells. *J Biosci Bioeng* 105:300-302
- 13 Thompson CJ, Movva NR, Tizard R, Cramer R, Davies JE, Lauwereys M, Botterman J  
14 (1987) Characterization of the herbicide-resistance gene bar from *Streptomyces  
15 hygrosopicus*. *EMBO J* 6:2513-2518
- 16 Tyczkowski JK, Hamilton PB (1986) Absorption, transport, and deposition in chickens of  
17 lutein diester, a carotenoid extracted from Marigold (*Tagetes erecta*) petals. *Poultry  
18 Sci* 65:1526-1531
- 19 Valot B, Langella O, Nano E, Zivy M (2011) MassChroQ: A versatile tool for mass  
20 spectrometry quantification. *Proteomics* 11:3572–3577
- 21 Vershinin A (1999) Biological functions of carotenoids—diversity and evolution.  
22 *Biofactors* 10:99-104
- 23 Yamagata T, Kato H, Kuroda S, Abe S, Davies E (2003) Uncleaved legumin in developing  
24 maize endosperm: identification, accumulation and putative subcellular localization. *J  
25 Exp Bot* 54:913-922
- 26 Zhong YJ, Huang JC, Liu J, Li Y, Jiang Y, Xu ZF, Sandmann G, Chen F (2011) Functional  
27 characterization of various algal carotenoid ketolases reveals that ketolating  
28 zeaxanthin efficiently is essential for high production of astaxanthin in transgenic  
29 *Arabidopsis*. *J Exp Bot* 62:3659-3669
- 30 Zhu C, Naqvi S, Breitenbach J, Sandmann G, Christou P, Capell T (2008) Combinatorial  
31 genetic transformation generates a library of metabolic phenotypes for the  
32 carotenoid pathway in maize. *Proc Natl Acad Sci USA* 105:18232–18237
- 33  
34

**Table 1** Carotenoid composition in kernels and endosperm of maize varieties and astaxanthin accumulating lines.Carotenoids ( $\mu\text{g/g}$  dw) in maize seeds and endosperm (-End)

	Ast	KetoZ	Viol	Lut	Zeax	aCry	bCry	bCar
M37W	--	--	1.02+0.25	0.56+0.04	2.53+0.32	--	--	--
M37W-End	--	--	1.06+0.28	0.84+0.04	2.65+0.43	--	--	--
NSL76	--	--	1.45+0.13	10.81+0.55	1.41+0.25	--	--	--
NSL76-End	--	--	0.43+0.05	12.71+1.57	1.23+0.11	0.43+0.08	0.28+0.05	--
M37bkt	10.76+1.56	6.47+0.16	--	2.49+0.49	6.83+1.30	0.42+0.17	2.00+0.86	1.30+0.66
M37bkt-End	11.14+1.88	7.82+0.55	--	2.84+0.89	7.22+1.29	0.55+0.20	1.96+0.47	1.18+0.54
NSL76bkt	16.77+1.45	4.97+0.93	--	1.08+0.18	2.56+0.52	0.33+0.10	0.62+0.18	1.80+0.43
NSL76bkt-End	15.67+2.18	8.32+0.14	--	--	6.70+1.47	0.02+0.005	2.07+0.49	2.27+0.87

-----

-- below detection; at least 3 independent samples, mean  $\pm$  SD; -End refers to isolated endosperm; dw: dry weight

Ast, astaxanthin; KetoZ, keto zeaxanthin; Viol, violaxanthin, Lut, lutein; Zeax, zeaxanthin; aCry,  $\alpha$ -cryptoxanthin, bCry,  $\beta$ -cryptoxanthin; bCar,  $\beta$ -carotene;

**Table 2** Metabolite ratios in maize kernel endosperm 30 DAP of NSL76-bkt versus NSL76

Metabolites	Ratio NSL76-bkt /NSL76
Sucrose	>10
Lactic acid	11.42 ±1.658
Malic acid	0.173 ±0.02
Gluconic acid	0.07 ±0.0005
Glycine	<0.1
Serine	<0.1
Glyceric acid	<0.1
Leucine	<0.1
Valine	<0.1
Alanine	<0.1
Aspartic acid	<0.1
Threonine	<0.1
Fumaric acid	<0.1
Succinic acid	<0.1
Glutamic acid	<0.1
Proline	<0.1

Data from three technical and two biological replicates, all with significance  $p < 0.05$

Table 3A "Proteins from endosperm derived from mature seeds

Accession	Description	GO Annotation of biological process and molecular function	Fold change NSL76-bkt / NSL76*
tr B6SMR2	MAIZE Peroxidase	GO:0006979: response to oxidative stress, GO:0004601: peroxidase activity GO:0016491: oxidoreductase activity	2.00
GRMZM2G180172_P01	A0A096T2V8- Uncharacterized protein		1.59
tr COHHY2	Uncharacterized protein	GO:0008152: metabolic process GO:0016311: dephosphorylation GO:0003993: acid phosphatase activity GO:0016787: hydrolase activity (IEA)	1.54
tr B6SKP5	Osmotin-like protein	---	0.67
tr B6TK50	beta-catenin-like repeat family protein	---	0.65
tr COPB51	Uncharacterized protein	GO:0008152: metabolic process GO:0016788: hydrolase activity, acting on ester bonds	0.63
tr B6SLL8	Malate dehydrogenase	GO:0005975: carbohydrate metabolic process GO:0006099: tricarboxylic acid cycle GO:0006108: malate metabolic process	0.63
tr K7US98	Chloroplast protein synthesis	---	0.63
GRMZM2G052175_P01	tr B6SZA3 - Endochitinase A	GO:0005975: carbohydrate metabolic process GO:0006032: chitin catabolic process GO:0016998: cell wall macromolecule catabolic process GO:0004568: chitinase activity (	0.63
sp P38560	Glutamine synthetase	GO:0006542: glutamine biosynthetic process GO:0006807: nitrogen compound metabolic process	0.61
tr Q41878	Sulfur-rich zein protein of Mr 15,000	---	0.59
tr K7VJF3	Uncharacterized protein	GO:0000166: nucleotide binding GO:0005524: ATP binding (IEA)	0.48
tr B6U4F7	Acylamino-acid-releasing enzyme	GO:0006508: proteolysis GO:0004252: serine-type endopeptidase activity)	0.40
tr B6SK46	Cupin family protein	GO:0045735: nutrient reservoir activity	0.34

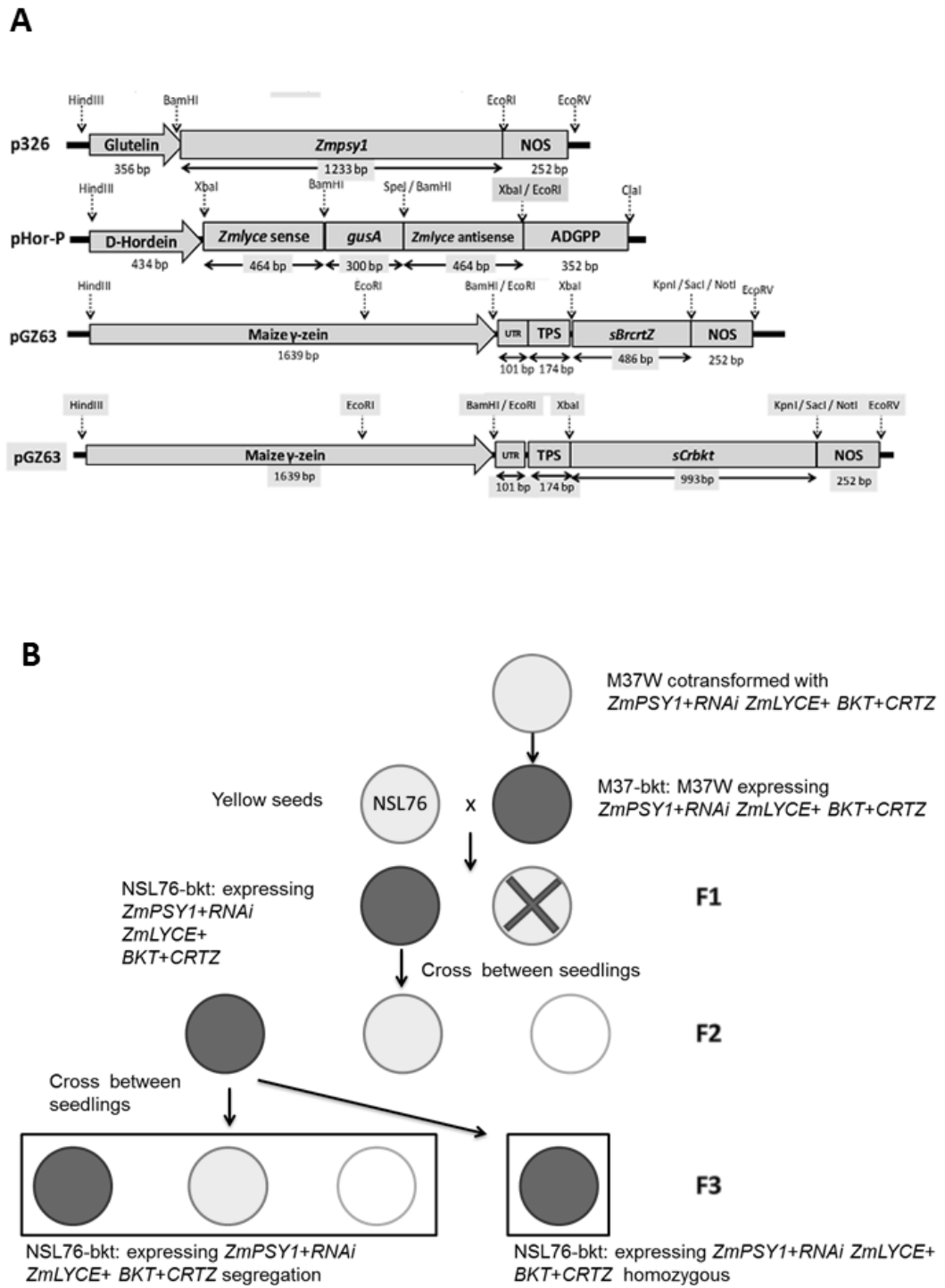
\*pWILCOX of 0.029

Table 3B Proteins from endosperm of seeds harvested 30days after pollination

Accession	Description	GO Annotation - Biological process and molecular function	Fold change NSL76-bkt / NSL76*
tr B6TFX9	Legumin-like protein	---	1.82
tr B6TNR5	Tetratricopeptide repeat protein KIAA0103	---	1.65**
tr B4FAZ6	Adaptin ear-binding coat-associated protein	GO:0000902: cell morphogenesis GO:0006858: extracellular transport GO:0006897: endocytosis, GO:0042626: ATPase activity GO:0016049: cell growth (IEA)	1.59**
GRMZM2G159142_P01	tr B6TX55 - Uncharacterized protein	---	1.54**
tr B6SJ37	Acyphosphatase = 1,3-diphosphoglycerate phosphatase	GO:0008152: metabolic process	0.67
tr K7VNE0	Uncharacterized protein	GO:0004611: phosphoenolpyruvate carboxykinase activity GO:0006094: gluconeogenesis	0.66
tr B4FZN6	40S ribosomal protein S7	GO:0006412: translation GO:0003735: structural constituent of ribosome	0.65
tr K7VWJ6	Uncharacterized protein	GO:0046872: metal ion binding	0.65
tr D2KLI5	Trehalose-6-phosphate synthase	GO:0005992: trehalose metabolism	0.65
GRMZM2G379758_P01	A0A096THR3 - Eukaryotic translation initiation factor 3 subunit C	GO:0001731: formation of translation preinitiation complex, GO:0006446: regulation of translational initiation	0.64
GRMZM2G067063_P02	tr Q5EUD1 - Protein disulfide isomerase	GO:0008152: metabolic process	0.63
tr B6UGM1	Prolamin PPROL 17	GO:0045735: nutrient reservoir activity	0.60
GRMZM2G007871_P01	A0A096PUR4 - Uncharacterized protein	GO:0031204: posttranslational protein targeting to membrane, translocation (	0.55
tr B6TZY1	Peroxiredoxin-5	GO:0055114: oxidation-reduction process	0.53
tr B6SY37	VHS and GAT domain protein	GO:0006886: intracellular protein transport	0.44
tr D2IQA1	Sucrose synthase	GO:0005985: sucrose metabolic process (IEA)	0.38
tr B8A2Z0	Uncharacterized protein	GO:0016831: carboxy-lyase activity	0.30

\*pWILCOX of 0.029 or \*\*0.042

Legends to figures



**Fig. 1** A. Transgene expression vectors for *ZmPSY1*, *RNAi-lyce*, *sBertZ* and *sCrbkt*. Abbreviations: NOS, nos terminator; ADGPP, ADP-glucose pyrophosphorylase

terminator; *sBrcrtZ*, truncated  $\beta$ -carotene ketolase (BKT); UTR, 5'-untranslated region of the rice alcohol dehydrogenase gene; TPS, transit peptide sequence from the *Phaseolus vulgaris* small subunit of ribulose bisphosphate carboxylase; *sCrBkt*, *CRTZ* gene encoding  $\beta$ -carotene hydroxylase.

B. Scheme describing the transformation of maize variety M37W yielding M37-bkt followed by crossing astaxanthin synthesis into the oil accumulating variety NSL76 and selection of high astaxanthin lines.



**Fig. 2** mRNA blot analysis of transgenes in corn endosperm at 30 DAP. Each lane was loaded with 30  $\mu$ g of total RNA. rRNA stained with ethidium bromide is shown as a control for loading of equal amounts of RNA.

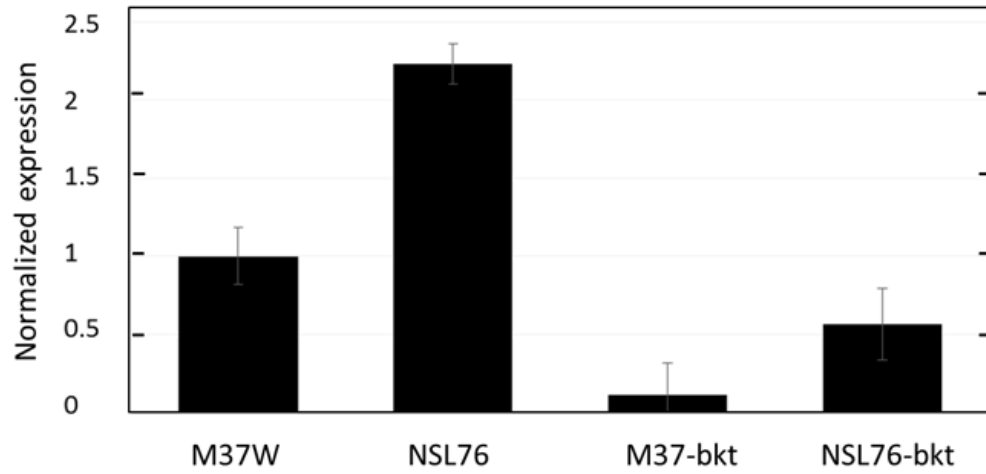


**Fig. 3** Transcript levels of endogenous *Zmlyce* gene in different maize lines.

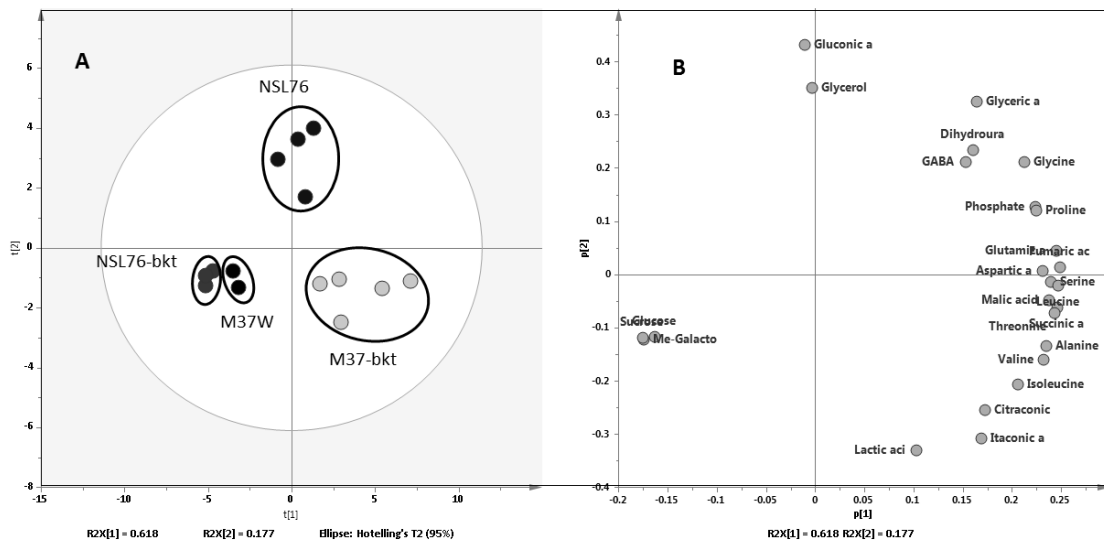


**Fig. 4** Principle component analysis of maize astaxanthin lines M37-bkt and NSL76-bkt and their parental lines M37W and NSL76. A. Score plot showing the clustering pattern; B. loadings plot showing the metabolites responsible for the clustering of these lines.